Published in final edited form as:
Cardiovasc Intervent Radiol. 2010 December ; 33(6): 1180–1185. doi:10.1007/s00270-010-9868-0.

Optimizing the Protocol for Pulmonary Cryoablation: A Comparison of a Dual- and Triple-Freeze Protocol

J. Louis Hinshaw,
Department of Radiology, University of Wisconsin, Mail Code 3252, 600 Highland Ave., Madison, WI 53792-3252, USA

Peter J. Littrup,
Department of Radiology, Karmanos Cancer Institute, 4100 John R St., Detroit, MI 48201, USA

Nathan Durick,
Department of Radiology, University of Wisconsin, Mail Code 3252, 600 Highland Ave., Madison, WI 53792-3252, USA

Winnie Leung,
Department of Radiology, University of Wisconsin, Mail Code 3252, 600 Highland Ave., Madison, WI 53792-3252, USA

Fred T. Lee Jr.,
Department of Radiology, University of Wisconsin, Mail Code 3252, 600 Highland Ave., Madison, WI 53792-3252, USA

Lisa Sampson, and
Department of Radiology, University of Wisconsin, Mail Code 3252, 600 Highland Ave., Madison, WI 53792-3252, USA

Christopher L. Brace
Department of Radiology, University of Wisconsin, Mail Code 3252, 600 Highland Ave., Madison, WI 53792-3252, USA

J. Louis Hinshaw: jhinshaw@uwhealth.org

Abstract

The purpose of this study was to compare a double freeze–thaw protocol to a triple freeze–thaw protocol for pulmonary cryoablation utilizing an in vivo porcine lung model. A total of 18 cryoablations were performed in normal porcine lung utilizing percutaneous technique with 9 each in a double- (10-5-10) and triple-freeze (3-3-7-7-5) protocol. Serial noncontrast CT images were obtained during the ablation. CT imaging findings and pathology were reviewed. No imaging changes were identified during the initial freeze cycle with either protocol. However, during the first thaw cycle, a region of ground glass opacity developed around the probe with both protocols. Because the initial freeze was shorter with the triple freeze–thaw protocol, the imaging findings were apparent sooner with this protocol (6 vs. 13 min). Also, despite a shorter total freeze time (15 vs. 20 min), the ablation zone identified with the triple freeze–thaw protocol was not significantly different from the double freeze–thaw protocol (mean diameter: 1.67 ± 0.41 cm vs. 1.66 ± 0.21

Correspondence to: J. Louis Hinshaw, jhinshaw@uwhealth.org.

Present Address: N. Durick, Advanced Radiology, SC, 615 Valley View Drive, Suite 202, Moline, IL 61265, USA
Present Address: W. Leung, 1155 Oriole Rd., Santa Barbara, CA 93108, USA

Conflicts of interest statement Fred Lee, M.D. is the cofounder and part owner of Neuwave Medical. Lisa Sampson is a consultant for Neuwave Medical. Chris Brace is a shareholder and consultant for Neuwave Medical.

cm, $P = 0.77$; area: 2.1 ± 0.48 cm^2 vs. 1.99 ± 0.62 cm^2, $P = 0.7$; and circularity: 0.95 ± 0.04 vs. 0.96 ± 0.03, $P = 0.62$, respectively). This study suggests that there may be several advantages of a triple freeze–thaw protocol for pulmonary cryoablation, including earlier identification of the imaging findings associated with the ablation, the promise of a shorter procedure time or larger zones of ablation, and theoretically, more effective cytotoxicity related to the additional freeze–thaw cycle.

Keywords

Interventional radiology; Radiofrequency ablation; Pulmonary

Introduction

Image-guided pulmonary ablation is a rapidly advancing technique that is being applied for the treatment of both primary lung cancer and limited metastatic disease to the lungs [1, 2]. Radiofrequency (RF) ablation has been the primary modality utilized in the clinical setting to this point. There also has been limited experience with microwave (MW) ablation and cryoablation [3]. It has been established through previous work that different tissues react differently to the application of ablative energies [4, 5]. The differences are primarily related to the local environment, including blood flow, the insulative properties of the surrounding tissues, electrical resistance (RF), and air flow among others. As these issues have become more apparent, there has been a movement toward developing specialized protocols for the ablation modalities based on the target tissue. The effect of target temperature, duration, and speed of both freezing and thawing cycles has been noted for many tumor and organ types [4], and the necessity of a triple-freeze cycle for more fibrous tumors or organ sites (such as the open cryotherapy techniques applied during curettage of bone tumors) suggests that there is a greater cytotoxic effect for each freeze cycle.

Cryoablation has been applied successfully in multiple tissue types, including prostate, breast, kidney, bone, and liver [6–10]. However, pulmonary cryoablation has undergone very little critical scientific evaluation, and as a result, many questions remain regarding its efficacy and applicability in the lung. It is intuitive that the optimal protocol in an aerated tissue might be different from that in a solid tissue, but optimization is in the early stages of investigation. It has been noted that the CT findings of iceball formation in the lung parenchyma are difficult to appreciate until the initial thaw [3, 5]. At that time, an area of ground glass opacity develops and subsequently enlarges during the remainder of the ablation. The ground glass opacity represents a combination of pulmonary hemorrhage and alveolar filling with proteinaceous debris, and this finding can be clinically useful in monitoring the extent of the ablation during the subsequent freeze cycles [5]. The visualization of the iceball around the cryoprobe may be the dominant benefit of cryotherapy compared with heat-based ablation because it can be used to guide the ice margin ~ 1 cm beyond visible tumor margins [4, 6, 11].

Multiple freezes also may have an important effect on the associated ablation. As pulmonary fluid fills the alveolar spaces after the first thaw, the thermal conductivity increases 20-fold (i.e., thermal conductivity: 0.024 for air vs. 0.58 for water and 0.49–0.5 W/mK for blood). This may actually result in more rapid formation of the iceball on subsequent freeze cycles, thereby also expanding the cytotoxic isotherm for more thorough cell kill throughout the visualized ablation zone.

The purpose of this study was to determine whether a triple-freeze protocol will allow more rapid visualization of the iceball extent for improved monitoring of the ablation zone and

whether this protocol results in faster and larger ablation zones in the pulmonary parenchyma.

Materials and Methods

Study approval was obtained from the Research Animal Care and Use Committee of our institution, and all husbandry and experimental studies were compliant with the National Research Council's Guide for the Care and Use of Laboratory Animals.

Three female domestic swine (approximate weight 68 ± 4.5 kg) were used for our study. Preanesthetic sedation was achieved with intramuscular tiletamine hydrochloride/ zolazepam hydrochloride 7 mg/kg (Telazol; Fort Dodge, IA) and xylazine hydrochloride 2.2 mg/kg (Xyla-Ject; Phoenix Pharmaceutical, St. Joseph, MO). Atropine 0.05 mg/kg (Phoenix Pharmaceutical, St. Joseph, MO) was provided to facilitate intubation. Endotracheal intubation was initially performed in the standard fashion. Anesthesia was induced and maintained with inhaled isoflurane (Halocarbon Laboratories, River Edge, NJ). Clinically available 1.7-mm cryoprobes were utilized for all ablations (Endocare, Inc., Irvine, CA). Once the animals were stabilized, they were placed in the prone position in the CT gantry and a planning noncontrast CT scan was performed through the chest. Two locations in each lower lobe and a single location in the each middle lobe were identified for cryoprobe placement and six Perc-17 Endocare cryoprobes were placed utilizing CT fluoroscopy, three in each lung. The location for the placement of the cryoprobes was determined based on a planning CT scan performed with a skin marker in place on both sides. The angle and depth of the cryoprobe placement was then determined and the cryoprobes were positioned with the aid of intermittent CT fluoroscopy. The cryoprobes were positioned within aerated lung parenchyma at least 2 cm from large bronchi or vessels and at least 5 cm apart. The ablations were randomized to one of two protocols. The first protocol was a double freeze–thaw cycle, consisting of a 10-min freeze, 5-min thaw, and 10-min freeze. The triple-freeze protocol was arbitrarily chosen to maintain the same total procedure time, which required shorter total freeze duration but consisted of a 3-min freeze, 3-min thaw, 7-min freeze, 7-min thaw, and 5-min freeze, which was based on anecdotal current clinical observations. This also allowed the same total procedure time of 25 min but only 15-min total freeze time for the triple freeze protocol. Noncontrast CT images were obtained 3, 6, 10, 13, 15, 20, and 25 min into the ablation. The final CT was performed with thin section technique (2.5-mm slice width with 1-mm overlap) to allow for multiplanar reconstruction of the images in a plane transverse to the cryoprobe. All ablation procedures were performed under the direction of a single operator who has extensive clinical and laboratory experience with ablation techniques. There were a total of 18 ablations performed, 9 in each group.

Immediately after the ablations, the pigs were sacrificed by means of an intravenous injection of Beuthanasia-D (390 mg/ml pentobarbital sodium and 50 mg/ml phenytoin sodium at 0.2 ml/kg IV; Schering-Plough, Kenilworth, NJ). The lungs were removed and the ablations sectioned transverse to the cryoprobe insertion track in approximately 5-mm increments. Sections were optically scanned as electronic files for later measurement. A representative slice from each ablation zone was measured by consensus between two of the authors using the software ImageJ. Measurements included minimum and maximum diameter, area, and circularity (4π (area/perimeter^2), i.e., a ratio that describes how close an object is to a perfect circle (1.0)).

Samples were stained with hematoxylin and eosin for histological evaluation. A slice that best showed complete ablation was selected and immediately stained with triphenyltetrazolium chloride (TTC) for better demarcation of the zone of complete necrosis [6]. A board-certified pathologist with extensive experience in evaluating tissue after

ablation performed histological and pathological evaluations. The CT images from the final acquisition were reconstructed in a plane transverse to each cryoprobe and the area, and diameter of the imaging changes indicative of the iceball and thus the ablation were measured.

Continuous data were expressed as means with standard deviations. A paired *t* test was performed to compare the two groups. A P value < 0.05 was considered to indicate statistical significance.

Results

Ablation was technically successful at all 18 sites in the 3 animals. A <10% pneumothorax with no associated symptoms was encountered in one animal, but there were no other complications.

Imaging Findings

Double Freeze—Thaw Protocol—No imaging changes were identified in the pulmonary parenchyma surrounding the cryoprobes during the initial 10-min freeze time. During the subsequent 5-min thaw, a halo of ground glass opacity with a denser halo around the outer rim developed around the cryoprobes, enlarging during the course of the thaw (Fig. 1A). During the second freeze, the ground glass opacity and outer halo expanded and increased in density. The density of the iceball remained less than 0 HU, presumably from a combination of the air trapped within the ice and the lower density of ice itself that formed within the edematous/hemorrhagic halo around the cryoprobe during the thaw. Centrally around the cryoprobe, a second area of relatively dense attenuation developed (13- and 15-min images in Fig. 1A). The border of the ablation zone beyond the iceball was variable in width and irregular along its border, presumably representing the nonfrozen extent of pulmonary hemorrhage/edema.

Triple Freeze—Thaw Protocol—With this protocol, no imaging changes were identified during the initial short 3-min freeze, similar to the first freeze in the double-freeze protocol (Fig. 1B). However, ground glass opacity developed around the cryoprobe during the initial 3-min thaw. As a result, the imaging changes associated with the iceball formation could be visualized on CT as early as 6 min with this protocol. During the subsequent second and third freeze, the iceball took on a targetoid appearance with a double halo around the periphery and a dense central region (Fig. 1B).

Pathology Findings

There was no significant difference in the ablation zone size between the two groups based on the gross pathology diameter (1.67 ± 0.14 cm vs. 1.66 ± 0.21 cm, $P = 0.77$), cross-sectional area (2.1 ± 0.48 cm^2 vs. 1.99 ± 0.62 cm^2, $P = 0.70$), or circularity of the ablation zones (0.95 ± 0.04 vs. 0.96 ± 0.03, $P = 0.62$). The ablation zone identified at pathology was, as expected, smaller than the iceball seen during the imaging. Based on the relative size of the iceball and the zone of ablation seen in this study, the zone of cellular necrosis is approximately 4–5 mm inside the edge of the iceball (iceball size minus zone of ablation divided by 2) and is essentially the same for both protocols (4.1 mm for the double freeze and 4.6 mm for the triple freeze). The total ablation procedure time was identical (25 min) between the two protocols, but the total freeze time for the triple freeze protocol was shorter (15 min) compared with the double-freeze protocol (20 min) with more time devoted to thawing in the triple freeze protocol.

Histology of the ablation zone with both protocols showed four distinct zones that have been previously described by our group (Hinshaw JL et al., presented at the 2008 annual meeting of the Radiological Society of North America and accepted for publication in the *Journal of Interventional Oncology*) [5]:

1. Zone A, which was composed of lung parenchyma showing extensive edema and dissolution of alveolar septae and composed of cells with pyknotic nuclei;
2. Zone B, where the lung parenchyma showed extensive edema and dissolution of alveolar septae similar to Zone A. In addition, there was air in ruptured coalesced alveolar spaces in this zone, explaining why this zone is less dense on imaging.
3. Zone C, which was very similar to Zone A, and appears to represent the manifestation of the halo/halos of increased attenuation on CT. Both the thick halo identified with the double-freeze protocol and the two thin halos identified with the triple freeze protocol had essentially identical histopathological findings.
4. Zone D, which was an area of intense hemorrhage centrally with disruption of alveolar walls and pyknotic nuclei in septal cells, but with a transition into more normal, likely viable cells more peripherally. The TTC staining confirmed cellular viability surrounding the ablation zone, but not within it (Fig. 2).

Comparison of the Double- and Triple-Freeze Protocols

The imaging findings of iceball formation were identified as early as 6 min with the triple-freeze protocol compared with approximately 13 min for the double-freeze protocol. The iceball size identified on imaging with the triple freeze protocol was 18.3 ± 0.1 mm, 20.6 ± 1.4 mm, and 25.9 ± 2.1 mm after 3, 10, and 15 min of freeze time. For comparison, the iceball size identified on imaging with the double freeze–thaw protocol was 20.7 ± 1.7 mm, 24.1 ± 2.1 mm, and 24.8 ± 2.3 mm after 10, 15, and 20 min of freeze time. Iceball size could not be assessed with either protocol before the initial thaw due to the lack of imaging findings. Despite a shorter overall freeze time, the iceball size for the triple-freeze protocol was slightly larger than for the double-freeze protocol, but the difference was not statistically significant (25.9 ± 2.1 mm vs. 24.8 ± 2.4 mm, $P = 0.3$). If you plot the iceball size versus total freeze time, the rate of iceball formation (i.e., slope of the line) is faster for the triple freeze protocol than it is for the double-freeze protocol (Fig. 3).

Conclusions

Our study shows that the triple-freeze protocol produces a zone of necrosis that is essentially identical to the double-freeze protocol despite a shorter overall freeze time (15 vs. 20 min). In addition, because an earlier thaw time is utilized in the triple-freeze protocol, the imaging changes associated with the iceball could be identified at 6 min rather than 13 min in the double-freeze protocol. Thus, the triple-freeze protocol may be more effective for intraprocedural monitoring of pulmonary cryoablation. In addition, the rate of iceball formation after the initial freeze seems to be greater with the triple-freeze protocol compared with the double-freeze protocol. This may be related to the formation of conducting ice and fluid/hemorrhage during the thaw, which should increase the thermal conductivity approximately 20-fold compared with the surrounding aerated lung parenchyma. It may be that this property of the triple-freeze protocol could be exploited to create even larger zones of ablation or to shorten the overall procedure time. More importantly, faster freeze rates are associated with greater cell lethality and generally correspond to larger cytotoxic zones within the same overall ice size [4]. This also may at least partially explain the equivalent zone of necrosis seen on acute histology despite the shorter overall freeze time with the triple freeze protocol (15 vs. 20 min). These encouraging observations suggest that the

greater complexity and cost of more detailed animal protocols appear justified to validate the potential greater efficacy of more rapid and cytotoxic freeze protocols.

The earlier visualization of the imaging changes associated with iceball formation can be clinically useful because this also defines the underlying cytotoxic isotherm (i.e., ~ −20 to −40°C), generally residing 5–10 mm behind the leading edge of visible ice and thus would allow intraprocedural monitoring of the zone of ablation [4, 6, 7, 11]. In our study, the cytotoxic isotherm appears to be approximately 4–5 mm inside the edge of the iceball, which is in agreement with previous studies. This ability to monitor the developing ablation zone should allow more accurate and safer ablations, especially when the target lesion is closely adjacent to sensitive structures, such as the esophagus, recurrent laryngeal nerve, and central airways [8]. With the emergence of more powerful cryoprobe technology, ice formation may need to be monitored more carefully and more frequently in the future. Of note, the thaw times were arbitrarily adjusted in our study so that the overall ablation time of the two protocols was the same. It may be possible to decrease the intervening thaw times and thus shorten overall procedure time, or allow more numerous freeze cycles in the same time.

This study represents an attempt to improve the protocol for utilization of cryoablation in the lung. The decision to use a triple-freeze protocol was based on clinical work and anecdotal reports that there was improved visualization and a potentially faster and larger ablation zone obtained by utilizing the triple-freeze protocol. Other studies of pulmonary cryoablation have suggested that either the current technology is suboptimal for application in the lung or that the applied protocols are suboptimal [4, 18]. Specifically, a study comparing cryoablation zone sizes in liver, kidney, and lung utilizing an identical double freeze–thaw protocol identified a smaller zone of necrosis within the lung [9], which did not even coalesce for sufficiently lethal temperatures between two probes. It is unclear whether this is because a nonoptimized protocol was utilized for pulmonary tissue, if there was an inherent flaw in their experimental model/technique, or if there is some inherent limitation to the application of cryoablation in normal tissue lung. Our study suggests that optimization of technique may improve the clinical efficacy of cryoablation in the lung, but also suggests that clinically relevant zones of ablation can in fact be achieved utilizing more accepted and established protocols.

One important factor that was not evaluated in this study is the interaction of the soft tissue target tumor within the lung and the adjacent aerated pulmonary parenchyma. This interface may have significant effects on the conductance of and distribution of thermal (in this case cryogenic) energy. It may be that the relatively poor thermal conductance of cytotoxic cold temperatures through aerated lung adjacent to a target tumor may result in a “freezer effect” within the tumor itself similar to the “oven effect” that has been described with heat-based ablation of hepatocellular carcinoma (HCC) in a cirrhotic liver [10]. If so, this may lead to lower and more cytotoxic temperatures within a targeted tumor than might otherwise be expected, yet still leave inadequate extension of ablation into the surrounding normal lung tissue to ensure a 1-cm margin. Evaluation in a large animal tumor model has been difficult to establish but may be necessary to evaluate these issues as we move forward.

Certain limitations of this study have already been noted. Our data are limited to a small sample size of only acute ablation, using single 1.7-mm probes in normal lung tissue. This approach is not representative of cryotherapy for clinical tumors that often require the use of at least two cryoprobes with the greatest freeze capacity, which are currently those with a 2.4-mm diameter. Optimization of the freeze and thaw components of cryotherapy protocols will need to continue in future studies. Nevertheless, the earlier visualization of potentially faster and more lethal iceball formation, even in normal lung tissue, suggests that additional

studies are not only warranted but are likely to lead to improved efficacy of lung cryotherapy protocols, in terms of both reduced procedure time and improved outcomes.

Percutaneous application of cryoablation in the lung is a burgeoning field with many as yet unanswered questions. One critical issue is optimization of each technology for application in the lung. Although this study does not resolve this question, it suggests that multiple freeze–thaw cycles, even if the overall freeze time is shorter, might be advantageous for optimizing both visualization and efficacy of cryoablation in the lung.

References

1. Suh RD, Wallace AB, Sheehan RE, Heinze SB, Goldin JG. Unresectable pulmonary malignancies: CT-guided percutaneous radiofrequency ablation—preliminary results. Radiology. 2003; 229:821–829. [PubMed: 14657317]
2. Simon CJ, Dupuy DE, DiPetrillo TA, et al. Pulmonary radiofrequency ablation: long-term safety and efficacy in 153 patients. Radiology. 2007; 243:268–275. [PubMed: 17392258]
3. Wang H, Littrup PJ, Duan Y, Zhang Y, Feng H, Nie Z. Thoracic masses treated with percutaneous cryotherapy: initial experience with more than 200 procedures. Radiology. 2005; 235:289–298. [PubMed: 15798173]
4. Gage AA, Baust J. Mechanisms of tissue injury in cryosurgery. Cryobiology. 1998; 37:171–186. [PubMed: 9787063]
5. Hinshaw JL, Durick NA, Leung W, et al. Radiology-pathology correlation of pulmonary cryoablation in a porcine model. J Interven Oncol. 2009; 2:113–120.
6. Littrup PJ, Ahmed A, Aoun HD, et al. CT-guided percutaneous cryotherapy of renal masses. J Vasc Interv Radiol. 2007; 18:383–392. [PubMed: 17377184]
7. Rewcastle JC, Sandison GA, Muldrew K, Saliken JC, Donnelly BJ. A model for the time dependent three-dimensional thermal distribution within iceballs surrounding multiple cryoprobes. Med Phys. 2001; 28:1125–1137. [PubMed: 11439482]
8. Ahmed A, Littrup P. Percutaneous cryotherapy of the thorax: safety considerations for complex cases. AJR Am J Roentgenol. 2006; 186:1703–1706. [PubMed: 16714662]
9. Permpongkosol S, Nicol TL, Link RE, et al. Differences in ablation size in porcine kidney, liver, and lung after cryoablation using the same ablation protocol. AJR Am J Roentgenol. 2007; 188:1028–1032. [PubMed: 17377040]
10. Liu Z, Ahmed M, Weinstein Y, Yi M, Mahajan RL, Goldberg SN. Characterization of the RF ablation-induced “oven effect”: the importance of background tissue thermal conductivity on tissue heating. Int J Hypertherm. 2006; 22:327–342.
11. Littrup PJ, Freeman-Gibb L, Andea A, et al. Cryotherapy for breast fibroadenomas. Radiology. 2005; 234:63–72. [PubMed: 15550369]

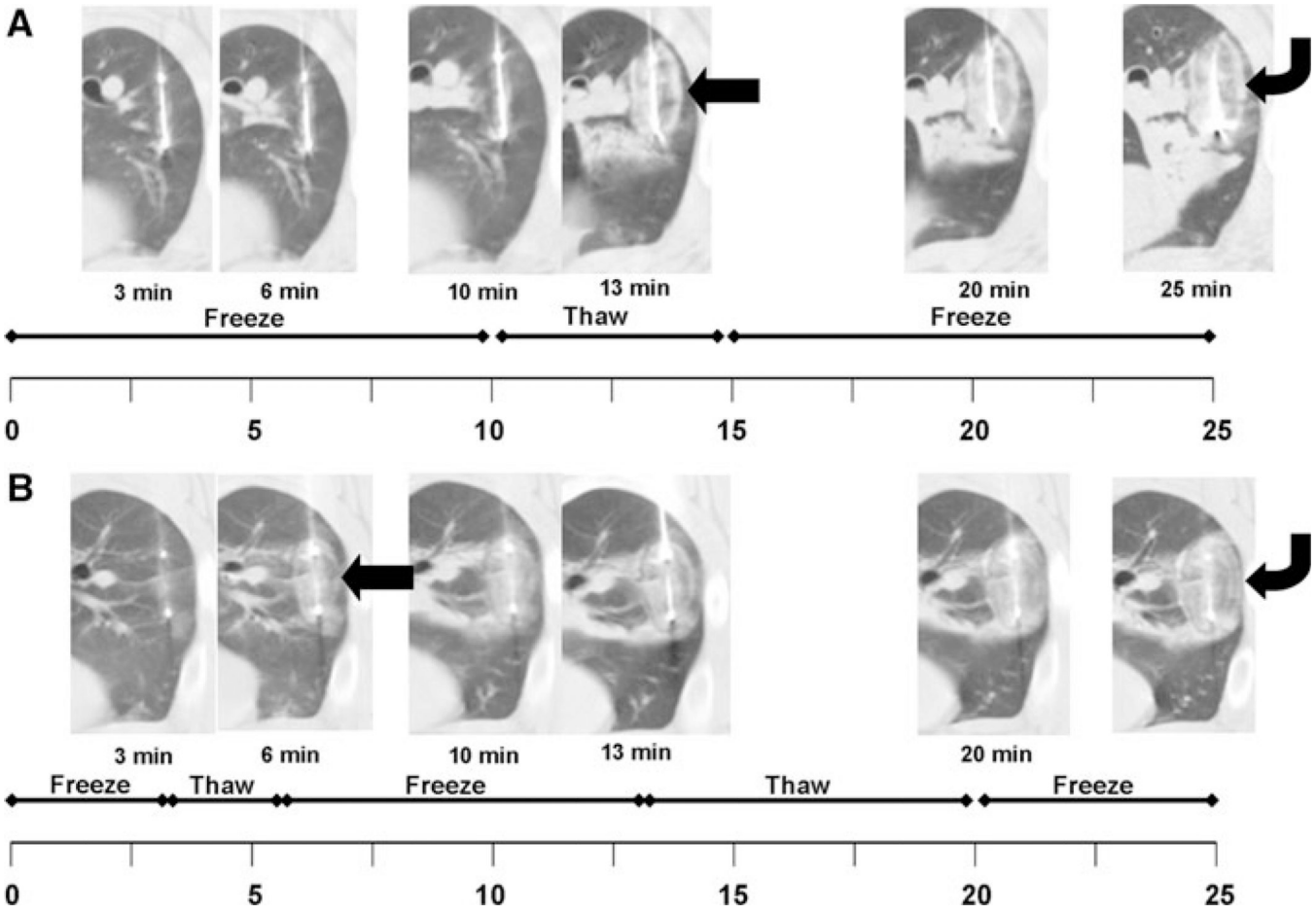

Fig. 1.

Timeline for both freeze protocols emphasizes the same total procedure time of 25 min but the double-freeze protocol uses 20 min total freeze time compared with only 15 min for the triple-freeze protocol. **A** In the double-freeze protocol, there are no imaging manifestations of the forming iceball until after the first thaw at 13 min (*arrow*, 13 min). At that time, you can see the ground glass attenuation representing the iceball with a single, thick outer halo, which becomes larger over time (*curved arrow*, 25 min). **B** In contrast, the forming iceball can be visualized at 6 min with the triple-freeze protocol (*curved arrow*, 6 min) and two thin halos form around the outer rim over time, presumably representing the layers of ice forming around the periphery (*curved arrow*, 25 min)

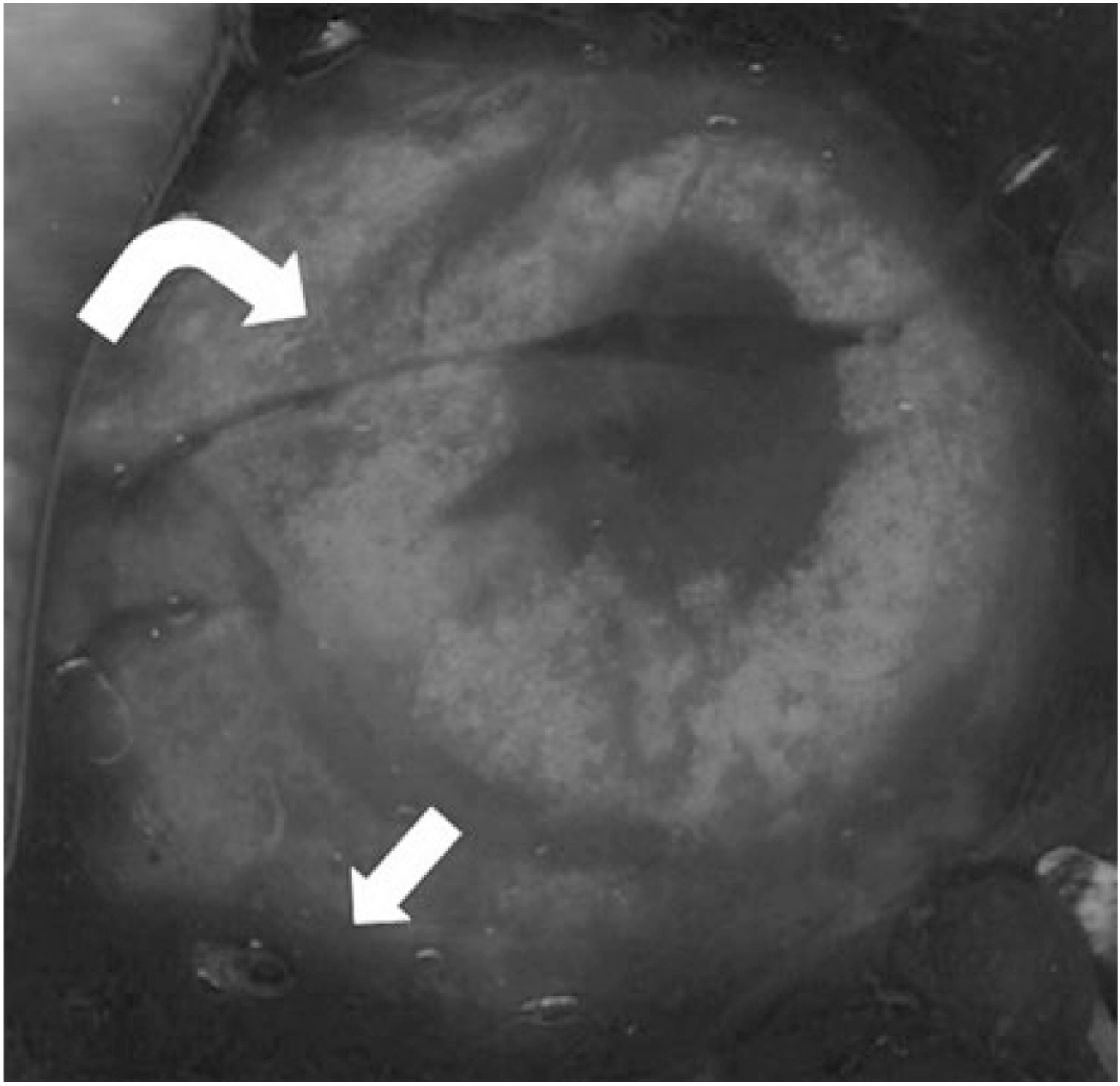

Fig. 2.

Gross pathology of a lung specimen from the triple-freeze protocol group, which was stained with triphenyltetrazolium chloride (TTC). The transition from nonviable tissue centrally to the darkly stained, viable tissue surrounding the ablation zone can be clearly seen (*arrow*). In addition, one can see the inner halo related to the triple-freeze protocol within the ablation zone (*curved arrow*). Although it was not directly studied, it is likely that the asymmetry in growth was related to central heat sinks, such as blood flow and air exchange, limiting the growth along the more central border

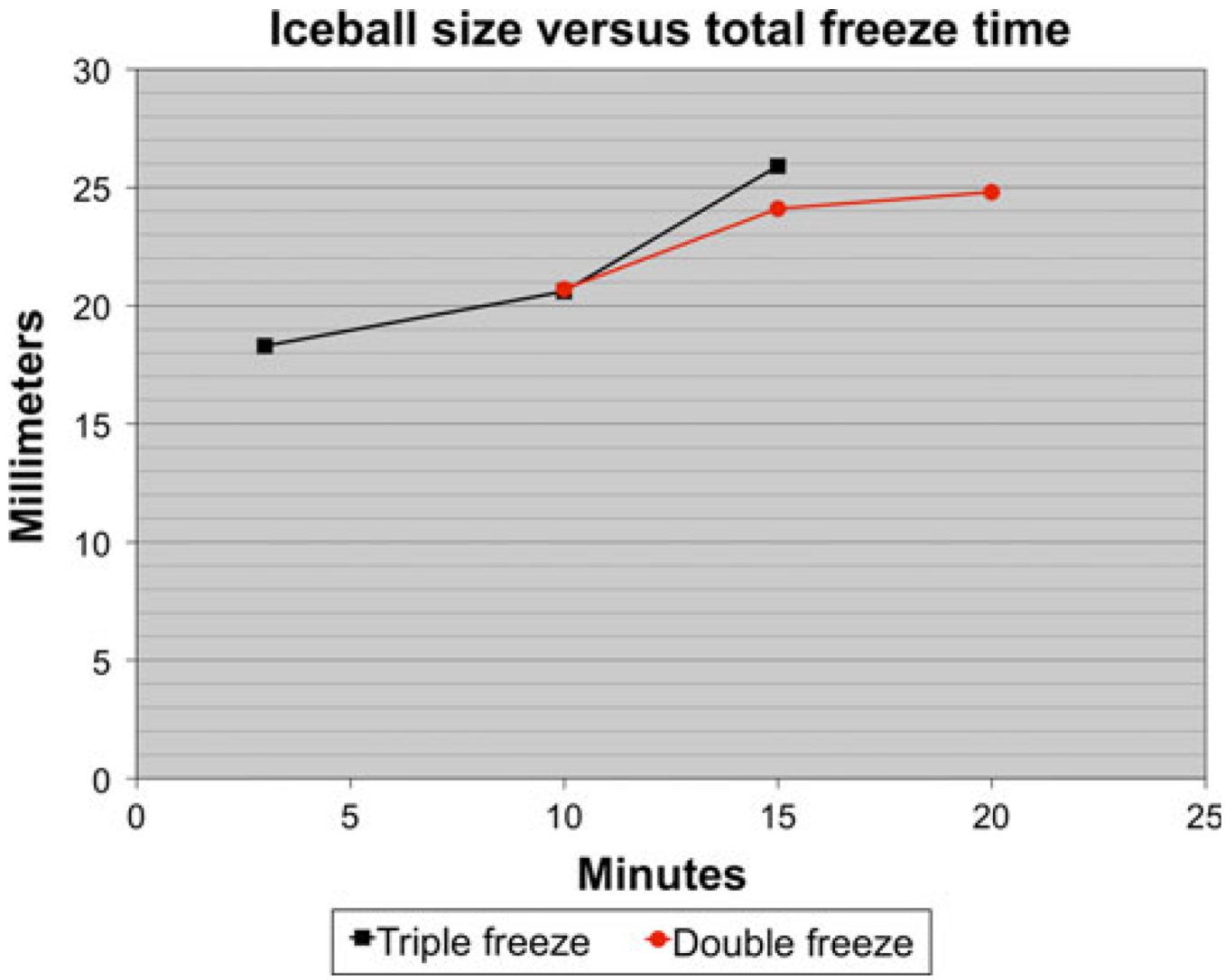

Fig. 3.

Graph plotting the size of the iceball seen on imaging versus the total freeze time rather than the total procedure time. There are two main findings on this graph. One is that the initial iceball formation appears to be relatively similar early in the procedure, resulting in an identical iceball size after 10 min of freezing. However, with the triple-freeze protocol, the rate of iceball formation (slope of the line) appears to increase in the third freeze resulting in more iceball growth in the final 5 min of the triple freeze compared with the final 10 min of the double freeze